J. Chem. Thermodynamics 55 (2012) 184–192

Contents lists available at SciVerse ScienceDirect

J. Chem. Thermodynamics

journal homepage: www.elsevier.com/locate/jct

Solubility of xylitol and sorbitol in ionic liquids – Experimental data and modeling

Aristides P. Carneiro, Oscar Rodríguez, Eugénia A. Macedo *

LSRE – Laboratory of Separation and Reaction Engineering – Associate Laboratory LSRE/LCM, Faculdade de Engenharia, Universidade do Porto Rua Dr. Roberto Frias, 4200-465 Porto, Portugal

ARTICLE INFO

Article history:
Received 30 March 2012
Received in revised form 3 May 2012
Accepted 18 May 2012
Available online 28 May 2012

Keywords:
Ionic liquids
Sugar alcohols
Solubility
Density
G^E models

ABSTRACT

Solubility of biomass-derived compounds in ionic liquids is an important parameter for the design of future processes incorporating ionic liquids as solvents for biorefining. Sugar alcohols such as sorbitol and xylitol are carbohydrate derivatives which have been identified as building blocks for biorefining. Therefore, in this work the solubility of these two sugar alcohols was measured experimentally within the temperature range of 288 K to 433 K, in three ionic liquids: [emim][$EtSO_4$], Aliquat®336 (*N*-Methyl-*N*,*N*-dioctyloctan-1-ammonium chloride), and Aliquat®[NO_3] (*N*-Methyl-*N*,*N*-dioctyloctan-1-ammonium nitrate). In addition, the densities of the ionic liquids were also measured and correlated. Local composition models such as NRTL, e-NRTL, and UNIQUAC were successfully applied to represent the experimental solubility data. The thermodynamic functions of dissolution were also calculated from the experimental data.

1. Introduction

Our planet has been facing a set of changes resulting from the continuous increasing on population growth as well as from society's development. These changes are caused primarily due to the high extraction rate of fossil resources which have impact in economy, environment, politics, and in life quality of the population.

Consequently, having a concern with maintenance and management of natural resources, 170 states have signed in 2002 an action plan for the 21st century (Agenda 21), which implies a search for new solutions to decrease today's rapid consumption of fossil, non-renewable resources (petroleum, natural gas, coal, minerals) [1]. This global effort is essential for a transition towards a modern society based on sustainable resources [2], achieving a sustainable development. Alternative raw materials to produce both chemicals and energy can be found in biomass, the most abundant renewable biological resource on earth [3]: biomass is available in nature as forest resources, wood, agricultural crops such as switchgrass, corn, and soybeans, as well as in residues from processing these materials. The major compounds of biomass are cellulose, hemicellulose, lignin (these three forming the lignocellulosic biomass, where they are often found interlinked), and starch (that is present in many plants such as rice, corn, potatoes, etc.).

Harvested biomass cannot be directly processed into other products, therefore pre-treatment technologies are required to dissolve it and separate the biopolymers, setting them more accessible as usable fractions to further processing. Mosier *et al.* [4] have explained in detail the pre-treatment issues and showing the existent technologies to carry it out. As the biomass main components are separated, each one could be treated as a starting material for biorefining. Cellulose, hemicellulose, and starch can be hydrolyzed to produce sugars using acidic media or enzymatic catalysis [5,6]. As for lignin, it can be burned to produce energy, used as packaging material or processed into aromatic compounds [7]. The sugars obtained from the hydrolysis of the polysaccharides are highly functionalized molecules and therefore available to react in many different ways: acetylation [8,9], dehydration [10,11], oxidation [12,13], and reduction [14].

Let us focus now on the reduction of sugars, mainly the hydrogenation under catalytic conditions of the carbonyl group, present in molecules such as glucose and fructose into a primary alcohol [15]. Such reduction yields a hydrogenated form of the carbohydrates: the sugar alcohols or alditols [16]. Sorbitol produced from glucose or fructose and xylitol yielded from xylose (both of them on batch technology) are among the most well known sugar alcohols and have a wide range of applicability not only directly in nutrition, cosmetic, and medicine, but also as high potential building blocks for a huge panoply of chemicals [17]. In addition, they have been considered two of the top twelve building blocks with higher potential to yield high-value bio-based chemicals or

Abbreviations: AARD, average absolute relative deviation; NRTL, non random two liquid; ILs, room temperature ionic liquids; LC, local composition contribution; PDH, Pitzer-extended Debye–Hückel contribution; UNIQUAC, Universal Quasi Chemical.

* Corresponding author. Tel.: +351 22 5081653; fax: +351 22 508 1674.
E-mail address: eamacedo@fe.up.pt (E.A. Macedo).

0021-9614/$ - see front matter © 2012 Published by Elsevier Ltd.
http://dx.doi.org/10.1016/j.jct.2012.05.020

Nomenclature

A_φ	Debye–Hückel parameter
a	slope of linear regression
b	y-axis intercept (density)
I	ionic strength
k	y-axis intercept (thermodynamic functions)
M	molar mass (g. mol^{-1})
N_p	number of experimental points
P	pressure
R	ideal gas constant (8.314 $J \cdot mol^{-1} \cdot K^{-1}$)
T	temperature (K)
V	volume
x	mole fraction

Greek letters

α	non-randomness parameter
β	thermal expansion coefficient
γ	activity coefficient
ΔC_p	heat capacity change ($J \cdot mol^{-1} \cdot K^{-1}$)
ΔG	Gibbs free energy change ($kJ \cdot mol^{-1}$)
ΔH	enthalpy change ($kJ \cdot mol^{-1}$)
ΔS	entropy change ($J \cdot mol^{-1} \cdot K^{-1}$)
ρ	density ($g \cdot mL^{-1}$)
ρ^*	closest approach parameter

Subscripts

2	related to the solute
dissol.	related to the dissolution process
fus	fusion
hm	harmonic mean
i	related to the i specie

Superscripts

0	standard state
Exp	experimental
L	liquid phase
model	calculated from the model

materials, according to the U.S. Department of Energy together with other institutions [17]. As stated in this report, sorbitol can be processed by catalytic dehydration, producing isosorbide (which can be used for the production of PET-like polymers), glycols used as antifreezers can be obtained by bond cleavage, and water-soluble polymers can be yielded by direct polymerization. As for xylitol, bond cleavage and direct polymerization are also applicable in its transformation, yielding the same sort of products (glycols and water-soluble polymers). In addition, xylaric and xylonic acids obtained from selective oxidation of xylitol can be used as additives for specialty formulation of concrete and cement [18].

Although these two sugar alcohols have a widespread spectrum of transformation, there are some barriers concerning the process engineering involving their production as well as their use as starting material. A new system of reaction media/catalyst might turn feasible a continuous process to yield these alditols with almost total conversion of starting sugars and high selectivity. Production of glycols, isosorbide and xylonic acid with higher yields as well as separation from some side products [17] are still some of the drawbacks which have to be solved, undergoing an economically feasible and more competitive biotransformation of biomass into chemicals. To face these challenges, a screening for solvents and catalysts for specific reactions and separations has to be made, in order to optimize the biorefining processes.

Room temperature ionic liquids (ILs), are a class of materials recently explored, with a wide range of applicability as solvents, catalysts, lubricants, etc. They have been defined as salts (once they are composed solely by ions) which are liquid at room temperature, or at least near to room temperature [19–22]. In general terms, they are characterized with unique properties such as negligible vapor pressure (non-volatility), wide liquid range, high thermal stability and conductivity, nonflammability, etc.

Other key feature of ILs is their tunability, *i.e.* small structural modifications either in the cation or in the anion, give rise to ILs with quite different physical properties and chemical affinity. This turns possible producing an ionic liquid that meets the specific characteristics needed for a given application. Due to all these reasons, they have been extensively exploited in the last twelve years, and the number of contributions has been increasing, covering issues about their synthesis [23], physical properties [24], applications in reaction and separation [25] engineering and modeling [26]. Despite its "boom" in the scientific community, industry has been slow in adopting ILs as reliable solutions for process design and engineering challenges [27], and few industrial processes are running so far. The high purchasing cost of ILs (despite it has been decreasing), the high viscosity which many of them have, and the lack of knowledge on physical properties, phase equilibrium data, and toxicity data, which albeit the efforts and the excellent contributions available in the literature, is still in development, have been appointed as the major barriers blocking the burgeon of ILs in industrial applications [27–29].

The potential use of ILs in biomass processing [7] has been demonstrated over the last years, and applications in biomass pre-treatment [30,31], hydrolysis of the biopolymers [32–34] and transformation of sugar into building blocks [35,36] have found in ILs a friendly way for lowering the energetic demand and equipment cost that standard biomass processing entails, though ILs recycling is critical to maintain economical viability of every process using them. ILs ability to be used as versatile solvents for biomass processing is strongly related with the molecular interactions which can be present when they form a mixture. Biomass compounds, especially biopolymers, are difficult to dissolve in conventional solvents due to strong hydrogen bonding linking these compounds together and the combination of amorphous and crystalline regions [37]. Some ILs are able to disrupt these bonds between biomass compounds and therefore to dissolve them efficiently [38]. This capacity, connected with ILs inherent properties, make them suitable to be used as reaction media, catalysts and extraction solvents in biorefining applications. Thus, solubility data of biomass-related compounds in ionic liquids is of extreme importance to efficiently screen the ILs with major potential for specific processes and for process design and optimization. Similarly, models that can represent accurately these phase equilibrium data are very helpful for a faster computation of the phase equilibrium.

Hence, in this work the solubility of the sugar alcohols sorbitol and xylitol was measured within the temperature range of 288 K to 328 K in three ionic liquids: 1-ethyl-3-methylimidazolium ethylsulfate, [emim][$EtSO_4$], Aliquat®336 (a mixture of methyltrioctylammonium chloride and methyltridecylammonium chloride), and Aliquat®[NO_3] (the same cation mixture with nitrate as anion). As a complement, density of these ILs as function of temperature

was measured and compared with available literature data. Thermodynamic functions of dissolution were calculated from solubility experimental data, and the activity coefficient models NRTL [39], e-NRTL [40], and UNIQUAC [41] were used for data correlation.

2. Materials and methods

2.1. Materials

Aliquat®336 with 0.0386 of water mass fraction (measured through Karl–Fisher titration) and average molar mass of 442 g. mol^{-1}, was purchased from Acros Organics and used without further drying. 1-Methylimidazole and diethylsulfate (>0.99, Merck) and toluene (>0.9999, Fisher Scientific), were used in the synthesis of [emim][$EtSO_4$]. Sodium nitrate (0.999, Sigma), acetone (0.999, Labsolve) and n-hexane (>0.999, Panreac) were used in Aliquat®[NO_3] synthesis. Xylitol (0.99, Alfa Aesar) and D-(−)-sorbitol (0.999, Merck) were the solutes used in this work and they were dried in vacuum oven at 50 °C for several hours to remove moisture. A sample description of ionic liquids and sugar alcohols is provided in table 1, and their chemical structures are presented in figure 1. All purities are given in mass fraction.

2.2. Synthesis of 1-ethyl-3-methylimidazolium ethylsulfate [emim][$EtSO_4$]

This IL was prepared according to a procedure available in literature [42] and briefly presented below. More details can be found in reference [43]. Equimolar amounts of 1-methylimidazole and diethylsulfate react under nitrogen atmosphere for 24 h at room temperature using toluene as solvent. After that, the IL phase was washed three times with fresh toluene, which is further removed by vacuum distillation. Traces of volatile compounds were removed by drying the IL for 48 h under vacuum at moderate temperatures (343 K). The water content of the resulting ionic liquid was 960 ppm (Karl–Fisher titration).

2.3. Synthesis of Aliquat®[NO_3]

This synthesis was performed based on a procedure available in literature [44], although with a few modifications regarding the ionic liquid's purification.

About 94.0 g (0.213 mol) of Aliquat®336 heated at 373 K were added dropwise to $NaNO_3$ in a quite large excess (28.6 g) previously dissolved in 50 mL of deionized water. Ten milliliters of acetone were added for a faster phase separation. The mixture was stirred for 6 h at room temperature and after that two liquid phases were separated. To remove NaCl and unreacted $NaNO_3$ the IL phase was washed with deionized water (3 · 100 mL), followed by (3 · 100 mL) of n-hexane to remove the unreacted Aliquat®336. The ionic liquid is finally dried under vacuum at moderate temperatures (343 K) to remove traces of n-hexane and excess water. The duration of the drying step is dependent on the application which the IL will be used. In this case, for solubility experiments, highly viscous ILs should be avoided, thus, the obtained Aliquat®[NO_3] had 0.0185 (mass fraction) of water in its content, showing a reasonable viscosity to be used in the solubility experiments.

Additionally, the chloride anion content was measured with a Mohr method (adding some acetone to attain a homogenous

TABLE 1
Sample description.

Chemical Name	Source	Initial mass fraction purity	Purification method	Final mole fraction purity	Analysis method
[emim][EtSO4]	Synthesis*	Not measured	Distillation	0.999	Karl–Fisher Titration, ^{1}H NMR,^{13}C NMR
Aliquat®336[a,b]	Acros Organics	0.96	None		
Aliquat®[NO_3][c]	Synthesis*	0.96	Extraction	0.973	Karl–Fisher Titration, Mohr method, ^{1}H NMR,^{13}C NMR
Xylitol	Alfa Aesar	0.99	None		
D-(−)-Sorbitol	Merck	0.999	None		

[a] Commercial name, a mixture of methyltrioctylammonium chloride and methyltridecylammonium chloride, with the first as predominant. It was used as received due to very high viscosity in dried solutions and solid state observed at water mass fraction <0.01.
[b] *N*-Methyl-*N*,*N*-dioctyloctan-1-ammonium chloride (IUPAC name).
[c] *N*-Methyl-*N*,*N*-dioctyloctan-1-ammonium nitrate (IUPAC name).
* Synthesized in our lab.

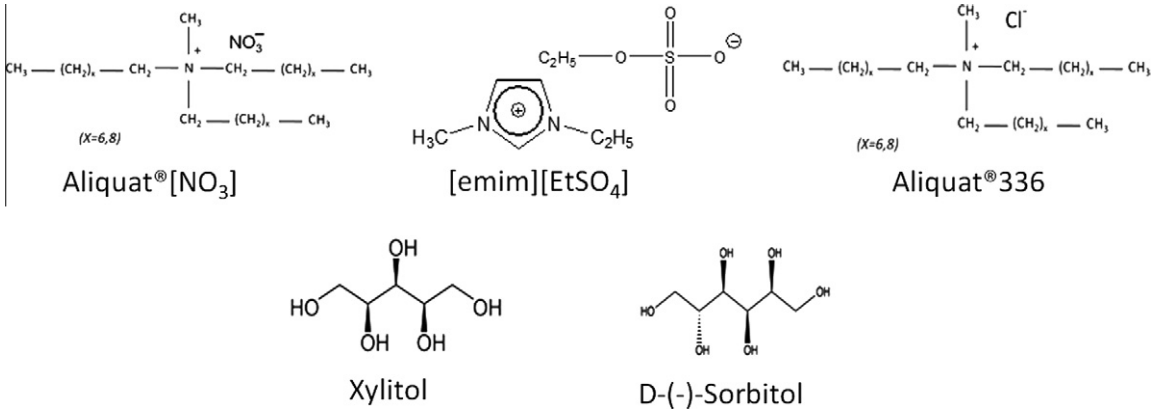

FIGURE 1. Chemical structures of the compounds.

aqueous solution to apply the test). The final chloride anion content was estimated in 0.008 (mass fraction). Finally, the chemical structure of the cation was checked by ^{1}H NMR, with results similar to the literature [44]. δ_H (400 MHz, $CDCl_3$) 0.87 (3H, q, $CH_2C\mathbf{H}_3$), 1.229 (2H, q, $CH_2C\mathbf{H}_2CH_2$), 1.662 (2H, s, N $CH_2C\mathbf{H}_2$), 3.149 (3H, s, $NC\mathbf{H}_3$), 3.303 (2H, t, $NC\mathbf{H}_2$).

2.4. Density measurements and solubility determination

Densities of the three ionic liquids were measured against temperature (±0.01 K), using a vibrating tube densimeter (Anton Paar DMA 4500 M), precise to within ±0.00001 g · mL^{-1}.

The solubility determination of xylitol and sorbitol in the ionic liquids, was performed using the setup described in detail in a previous work [43]. Briefly, it is an isothermal technique using a thermostatic bath (*JULABO F12-ED*) to control the temperature, flowing water through jacketed glass equilibrium cells. Solutes are added in a slight excess and magnetic stirring is applied until saturation. Preliminary experiments were made to estimate the time necessary to attain the phase equilibria. As in the previous work, 48 h of stirring were applied. After phase separation, small amounts of the clean saturated liquid phase are sampled in triplicate to quantify the solute. Quantification of xylitol and sorbitol was made using an isocratic HPLC method [43], with water as mobile phase flowing at 0.7 mL · min^{-1} through a (250 mm · 4 mm) column with RP-18 stationary phase. Detection was made using a continuous refractive index detector *HITACHI L-2490*.

3. Results and discussion

3.1. Density of the studied ionic liquids

The experimental density data for the three ILs used in this work are presented in table 2 and in figure 2.

The temperature range chosen in this work was determined by the temperature range in which the solubilities would be measured in the ionic liquids with tetraalkylammonium as cation (*i.e.* 308 K to 338 K), to allow these density data to be useful for modeling purposes (*i.e.* parameterization of thermodynamic models). Also it was affected by the relative higher melting temperatures of these two ionic liquids [44], hence densities below 293 K, were not measured. In the case of [emim][$EtSO_4$] a wide range of experimental density data is already available in the literature [45–48], thus, in this work its density was measured in a shorter temperature range (293 K to 323 K), only to evaluate the accuracy of density measurements performed.

TABLE 2
Experimental density data for the ionic liquids as a function of temperature at 101.3 kPa.

[emim][$EtSO_4$] w_{H_2O} = 0.00096[a]		Aliquat®336 w_{H_2O} = 0.0386[a]		Aliquat® [NO_3] w_{H_2O} = 0.0185[a]	
T/K	ρ/(g · cm^{-3})	T/K	ρ/(g · cm^{-3})	T/K	ρ/(g · cm^{-3})
293.16	1.24025	293.15	0.88947	293.16	0.91529
298.15	1.23681	298.14	0.88645	298.14	0.91233
303.15	1.23339	303.14	0.88343	303.14	0.90937
308.15	1.22998	308.14	0.88041	308.14	0.90641
313.15	1.22659	313.14	0.87737	313.14	0.90343
318.15	1.22322	318.14	0.87435	318.14	0.90050
323.18	1.21984	323.14	0.87136	323.14	0.89758
		328.14	0.86837	328.14	0.89467
		333.14	0.86537	333.14	0.89176
		338.14	0.86237	338.14	0.88884
		343.14	0.85936	343.14	0.88593

The uncertainty associated to the temperature measurement is: $u(T)$ = ±0.03 K.
The uncertainty associated to the density measurement is: $u(\rho)$ = ±1 · 10^{-5} g · cm^{-3}.
[a] Water content measured by Karl–Fisher titration in mass fraction.

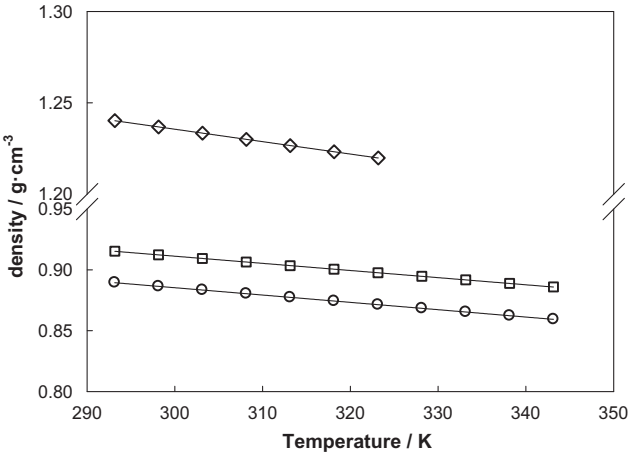

FIGURE 2. Experimental density ρ for the studied ionic liquids. [emim][$EtSO_4$], ○; Aliquat®336, □; and Aliquat®[NO_3], ◇.

Most of the ILs have room temperature densities above the water density (~1 g · mL^{-1}), being 1.2 g · mL^{-1} a kind of heuristic for ILs density. However, large cations such as Aliquat®, have densities lower than water. Reasons for that are the higher flexibility of their long alkyl chains, therefore a larger volume. As a result, lower densities are observed for these ILs, and many of them are less dense than water. Thus, supported in that explanation, it is quite easy to discuss the lower density of Aliquat's relatively to [emim][$EtSO_4$]. In order to compare the two ammonium based ILs, it must be kept in mind that, for the same cation, the density at a given temperature is related with the bulkiness of the anion anion [49–51]. Taking this into account, and as the bulkiness of nitrate anion (M = 62 g · mol^{-1}) is higher than chloride anion (M = 35.5 g · mol^{-1}), the density of Aliquat®[NO_3] is therefore higher (see figure 2). Nevertheless, the relative higher water content of these two ILs could also play an important role increasing the density. However, and as the higher water content is observed for Aliquat®336 (which is the less dense) the previous reasoning is still valid.

Figure 3 shows the comparison of the results obtained in this work with the density data available in the literature for these ionic liquids, in terms of the absolute deviation at each temperature. In the case of [emim][$EtSO_4$] these deviations were remarkably small, being lower than 0.001 g · mL^{-1} for all the data sets. For Aliquat®336 and Aliquat®[NO_3] slightly higher deviations were

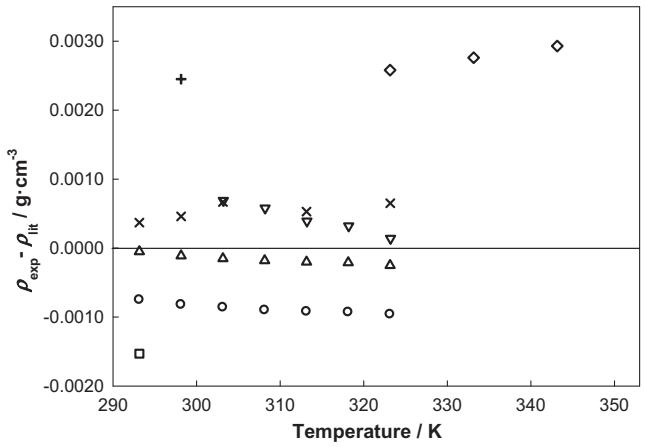

FIGURE 3. Absolute deviations between experimental density and literature data. Aliquat®336: reference [63], □, and information from supplier, +; Aliquat®[NO_3]: reference [44], ◇; and [emim][$EtSO_4$]: reference [45], ○, reference [46], △, reference [47], ▽, reference [48], ×.

TABLE 3
Parameters of linear regression of experimental density data.

Ionic liquid	$a \cdot 10^3/(g \cdot cm^{-3} \cdot K^{-1})$	$b/(g \cdot cm^{-3})$	r^2
[emim][$EtSO_4$]	−0.6798	1.4395	0.99998
Aliquat®336	−0.6021	1.0660	0.99999
Aliquat®[NO_3]	−0.5872	1.0874	0.99998

TABLE 4
Average isobaric thermal expansion coefficient and performance of density data correlation with equation (5).

Ionic liquid	$\beta \cdot 10^3/K^{-1}$	$\sigma \cdot 10^4$	ARD[a]
[emim][$EtSO_4$]	5.53	0.03	0.0011
Aliquat®336	6.89	0.08	0.0037
Aliquat®[NO_3]	6.52	0.07	0.0012

[a] $ARD(\%) = \frac{100}{N_p} \cdot \sum_{i=1}^{N_p} |\rho_{i,calc.} - \rho_{i,exp.}|/\rho_{i,exp.}$.

found (0.0029 $g \cdot mL^{-1}$ and 0.0024 $g \cdot mL^{-1}$, respectively), but literature data do not report information about water content in these ILs and visual interpolation had to be made for obtaining the density values. Therefore, the density data obtained in this work is in good agreement with literature data. Clearly, a linear decrease in density with temperature is observed for the three ILs. Hence, in figure 2 linear regressions of the density data are also plotted, which accurately describe the density of the ILs in the temperature range considered. Therefore equation (1) was used to correlate the density, ρ, with the temperature, T:

$$\rho = aT + b. \tag{1}$$

Table 3 shows the parameters a and b as well as the coefficient of determination, r^2, of the linear regressions.

For a given mass of pure fluid, at constant pressure, the volume can be differentiated as follows:

$$dV = \left(\frac{\partial V}{\partial T}\right)_P dT. \tag{2}$$

Or in terms of density,

$$d\rho = \left(\frac{\partial \rho}{\partial T}\right)_P dT. \tag{3}$$

The isobaric thermal expansion coefficient, β, is defined as:

$$\beta = -\frac{1}{\rho}\left(\frac{\partial \rho}{\partial T}\right)_P. \tag{4}$$

Combining the last two equations, and considering the temperature ranges for which β could be assumed constant, it results:

$$\rho = \rho_0 e^{(-\beta[T-T_0])}, \tag{5}$$

where ρ_0, is a known value of density at a temperature T_0. From the linear regressions, we can estimate an average β, for each IL valid for the temperature range studied as shown in table 4, together with its standard deviation, σ. Once this parameter is calculated, equation (5) can be used to compute the densities. Average relative deviations, *ARD*, between densities calculated from equation (5) and experimental data are also included in table 4, considering T_0 equal to 298 K and ρ_0 the density of each IL at this temperature. Calculated values of *ARD* presented in table 4, show high accuracy of equation (5) representing the experimental density data.

3.2. Solubility of xylitol and sorbitol in the ionic liquids

The obtained solubility data for the six binary systems are presented in table 5. Due to the high viscosities of Aliquat®336 and Aliquat®[NO_3], the temperature range of the solubility measurements for these two ionic liquids was set to 308 K to 343 K to avoid long dissolution stages. In the case of [emim][$EtSO_4$] the temperature range 288 K to 323 K was maintained relatively to the previous work [43]: the low viscosity of this IL allows efficient mixing at low temperatures (288 K). Figures 4 and 5 clearly show the solubility behavior of the two sugar alcohols in the three ILs, following in both cases the series: [emim][$EtSO_4$] > Aliquat®336 > Aliquat®[NO_3]. Hydrophobicity of Aliquat® cation causes weaker interactions between the ILs and the solutes, which are very polar and hydrophilic. As a result lower solubilities were obtained using the two ammonium based ILs, compared to those using the hydrophilic ionic liquid, [emim][$EtSO_4$]. Differences on solubility between the two Aliquat's, can be attributed, in one hand, to a higher water content in Aliquat®336 (allowing larger amounts of solute to be dissolved). On the other hand the higher Lewis basicity of chloride over nitrate anions provides a better ability to establish hydrogen bonds with the hydroxyl groups of xylitol and sorbitol. Although showing very similar behavior in the three ILs, sorbitol

TABLE 5
Experimental solubilities of carbohydrates in the ILs at 101.3 kPa.

[emim][$EtSO_4$]			Aliquat®336			Aliquat® [NO_3]		
T[a]/K	Sol. mass fraction	σ[b]	T/K	Sol. mass fraction	σ	T/K	Sol. mass fraction	σ
				Xylitol				
289.2	0.113	0.003	308.2	0.123	0.006	308.0	0.036	0.006
298.1	0.146	0.001	318.0	0.151	0.004	318.0	0.050	0.001
308.2	0.187	0.002	328.1	0.193	0.003	328.7	0.071	0.004
318.4	0.247	0.002	335.5	0.211	0.003	338.8	0.095	0.003
328.3	0.310	0.003	343.0	0.250	0.007	344.9	0.115	0.002
				Average standard relative uncertainty, u(Sol.)/Sol.				
±0.01			±0.01			±0.02		
				D-(−)-Sorbitol				
298.1	0.200	0.003	318.0	0.186	0.003	317.8	0.056	0.002
308.2	0.2283	0.0004	328.1	0.207	0.005	328.1	0.076	0.001
318.4	0.283	0.002	335.5	0.217	0.008	338.1	0.089	0.003
328.3	0.3377	0.0001	343.0	0.248	0.004	344.4	0.103	0.001
				Average standard relative uncertainty, [c] *u(Sol.)/Sol.*				
±0.02			±0.01			±0.02		

[a] The uncertainty associated to the temperature measurement is: $u(T) = \pm 0.01$ K.
[b] Standard deviation in mass fraction.
[c] The relative uncertainty regarding solubility is presented for each system as it depends on each calibration curve as well as on the solubility values.

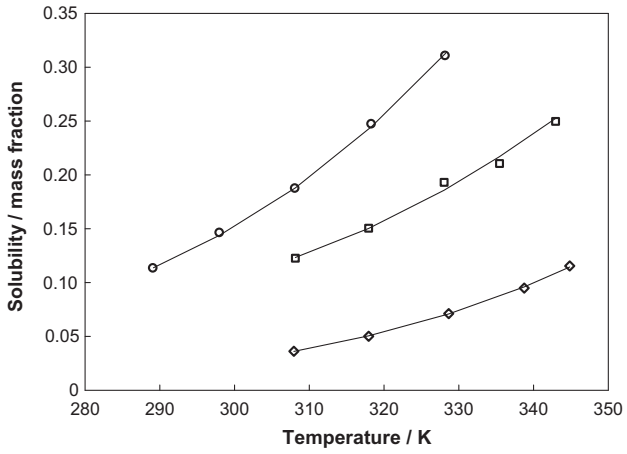

FIGURE 4. Experimental data and correlation of xylitol solubility in the three ILs. [emim][$EtSO_4$], ○; Aliquat®336, □; Aliquat®[NO_3], ◇; and eNRTL, –.

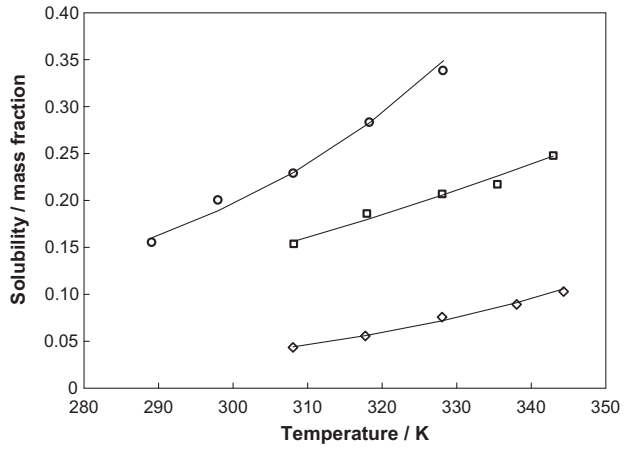

FIGURE 5. Experimental data and correlation of sorbitol solubility in the three ILs. [emim][$EtSO_4$], ○; Aliquat®336, □; Aliquat®[NO_3], ◇; and eNRTL, –.

is always more soluble than xylitol. An additional hydroxyl group seems to be sufficient to produce a significant difference on solubility in [emim][$EtSO_4$], in which solute–solvent interactions are stronger. In Aliquat®336 and Aliquat®[NO_3], the additional OH group does not play such an important role. The solubility of the two sugar alcohols can be related with their melting properties (table 6), since lower attraction between solutes and Aliquat ILs exists. As melting enthalpy is lower for sorbitol, its solubility is expected to be higher. To our knowledge, there are no available data in literature to compare the results obtained in this work.

3.3. Thermodynamic modeling

Local composition models have proved to be adequate for data correlation of carbohydrates' solubility in ILs [43]. In addition to the original NRTL [39], and UNIQUAC [41] models, the electrolyte version of NRTL, e-NRTL, was also applied here to compare its performance with the original NRTL version. First developed in 1982 by Chen *et al.* [40], the e-NRTL has two contributions for the activity coefficient of a species in solution: an NRTL-type local composition contribution, γ_i^{LC}, and a Pitzer-extended Debye–Hückel contribution, γ_i^{PDH} which assumes different expressions whether calculating activity coefficients for molecular species or ionic species. In this work, only activity coefficients for the solute (which is expression used to calculate the Pitzer-extended Debye–Hückel contribution is the following:

$$\ln \gamma_i^{PDH} = \frac{2A_\varphi I_\chi^{2/3}}{1+\rho^* I_\chi^{1/2}}, \tag{6}$$

where ρ^*, stands for the closest approach parameter which is normally set to 25 for ionic liquids [54,55]. A_φ and I_χ are the Debye–Hückel parameter and the ionic strength in molar basis respectively. Expressions to calculate them are presented in detail in reference [54].

The resulting equation for the activity coefficient is given by:

$$\ln \gamma_i = \ln \gamma_i^{LC} + \ln \gamma_i^{PDH}. \tag{7}$$

Both contributions have different expressions whether in case of ionic or molecular species. Solubility is usually modeled through the (solid + liquid) equilibria equation which is generally obtained through an idealized thermodynamic cycle [56] while applying some assumptions:

(i) solid phase is composed of pure solute;
(ii) solute's heat capacity difference between pure liquid and solid is considered temperature independent.

This derivation results in the following expression to compute the solubility, x_2^L, as a function of temperature, T:

$$\ln(x_2^L \cdot \gamma_2^L) = \frac{\Delta H_2^{fus}}{RT_2^{fus}}\left(1-\frac{T_2^{fus}}{T}\right) - \frac{\Delta C_{P2}^{fus}}{R}\left[\left(1-\frac{T_2^{fus}}{T}\right)+\ln\left(\frac{T_2^{fus}}{T}\right)\right]. \tag{8}$$

Activity coefficients of solute in liquid phase, γ_2^L, are calculated with a suitable thermodynamic model. Melting temperature, T_2^{fus}, enthalpy, ΔH_2^{fus}, and heat capacity difference for the solute, ΔC_{P2}^{fus}, should be known or at least estimated to apply equation (8). Regarding e-NRTL, its symmetric version [57] was adopted here applying equation (6) for the long range interactions. As the goal in this work is to compute the activity coefficient of molecular solutes in the liquid phase, the expressions to calculate activity coefficients of ions were not needed, turning the approach simpler than for (liquid + liquid) equilibria [54].

UNIQUAC structural parameters r and q for each component were found in the literature for the solutes and [emim][$EtSO_4$]. For Aliquat®336 and Aliquat®[NO_3], the empirical correlation proposed by Domanska and Mazurowska [58] was applied. Table 7 presents the structural parameters used in this work for UNIQUAC model. The binary interaction parameters for each model were adjusted by minimization of the average absolute relative deviation, AARD:

TABLE 6
Properties of the sugar alcohols used in this work.

Solute	M1 ($g \cdot mol^{-1}$)	T_{fus}/K	$\Delta_{fus}H$/($kJ \cdot mol^{-1}$)	$\Delta_{fus}C_p$/($J \cdot mol^{-1} \cdot K^{-1}$)	Reference
Xylitol	152.15	367.52	33.68	100[a]	[52]
D-(−)-Sorbitol	182.14	370.85	30.20	155.4[b]	[53]

[a] Estimated based on data for solid state and liquid state from reference [52].
[b] Estimated based on data for solid state and liquid state from reference [53].

TABLE 7
Structural parameters used in UNIQUAC model.

Compound	$M/(g \cdot mol^{-1})$	r	q	Reference
[emim][$EtSO_4$]	236.3	23.12	14.36	[59]
Aliquat®336	442	14.60	11.68	[a]
Aliquat®[NO_3]	468.6	15.04	12.03	[a]
xylitol	Table 2	5.34	4.68	[60]
sorbitol		6.31	5.50	[60]

[a] This work.

$$AARD(\%) = 100 \cdot \sum_{i=1}^{N} \frac{\left| x_{2,i}^{L,exp} - x_{2,i}^{L,model} \right|}{x_{2,i}^{L,exp}}. \quad (9)$$

Once models' parameters are obtained, they can be used to compute activity coefficients as a function of T and x_2^L. Thus together with equation (8), the value of x_2^L is calculated as a root of that equation.

Table 8 presents the performance of the three thermodynamic models correlating the solubility data, as well as the binary interaction energies, Δg_{ij} for NRTL and e-NRTL and Δu_{ij} for UNIQUAC. As done it is common practiced, the non-randomness parameter for NRTL, α, was set in 0.3 in most of the cases, except in the system Aliquat®336 with sorbitol were the value of 0.2 produced better results. These values were fixed according to the literature [61]. No significant differences in the accuracy of the three models were found. However, the electrolyte version of NRTL produces a slight improvement in almost all cases. Generally, all the three models represent quite well the experimental solubility data as shown in figures 4 and 5 and all the *AARDs* are below 4% as presented in table 8.

3.4. Apparent thermodynamic functions of dissolution

The thermodynamic behavior of dissolution process can be accessed through three thermodynamic functions: enthalpy of dissolution, $\Delta^0_{dissol.}H$, which indicates if the dissolution process releases or absorbs heat, Gibbs free energy change of dissolution, $\Delta^0_{dissol.}G$, which indicates whether the process is spontaneous or not, and entropy of dissolution, $\Delta^0_{dissol.}S$, that shows which is the more favorable state: the solution or the pure solvent. Note that these functions are apparent functions since they are obtained from experimental data. They are also important to estimate energetic parameters for equations of state to model the solubility data. The approach to calculate them is that proposed by Krug and coworkers [62], which is based on a modified Van't Hoff equation:

$$\left[\frac{\partial \ln x_2}{\partial\left(\frac{1}{T} - \frac{1}{T_{hm}}\right)}\right]_p = -\frac{\Delta^0_{dissol.}H}{R}, \quad (10)$$

where x_2 is the solubility of the solute in mole fraction, R is the ideal gas constant, T is the temperature in K, and T_{hm} is the harmonic average of the experimental temperatures given by:

$$T_{hm} = \frac{N_p}{\sum_{i=1}^{N_p} \frac{1}{T_i}}, \quad (11)$$

where N_p is the number of experimental data points. The enthalpy of dissolution, $\Delta^0_{dissol.}H$, is obtained from the slope of the linear plot of $\ln x_2$ against $(1/T - 1/T_{hm})$, as shown in figure 6. To calculate the change of Gibbs free energy during the dissolution, $\Delta^0_{dissol.}G$, this approach uses the following expression:

TABLE 8
Parameters and accuracy of each model on the correlation of experimental data.

Solute	Ionic liquid	NRTL[a]			UNIQUAC			eNRTL[a]		
		$\Delta g_{12}/R$ (K)	$\Delta g_{21}/R$	AARD %	$\Delta u_{12}/R$ (K)	$\Delta u_{21}/R$	AARD %	$\Delta g_{12}/R$ (K)	$\Delta g_{21}/R$	AARD %
Xylitol	[emim][$EtSO_4$]	−647.4	813.0	0.9	−300.0	373.8	1.1	−2894.7	−332.7	0.8
	Aliquat®336	−600.7	2662.8	1.9	−345.3	995.3	1.9	−2811.8	−584.6	1.7
	Aliquat®[NO3]	−154.1	2399.2	1.2	−217.5	541.6	1.3	−2522.2	−236.9	0.7
Sorbitol	[emim][$EtSO_4$]	−553.0	723.6	2.5	−229.8	221.7	2.6	−3240.7	−462.4	2.6
	Aliquat®336	−638.6	4566.2[b]	2.7[b]	−332.5	919.9	2.9	−3444.8[b]	−548.1[b]	2.0
	Aliquat®[NO3]	−90.2	2140.6	3.7	−204.1	491.3	3.2	−2782.0	341.8	2.4

[a] $\alpha = 0.3$.
[b] $\alpha = 0.2$.

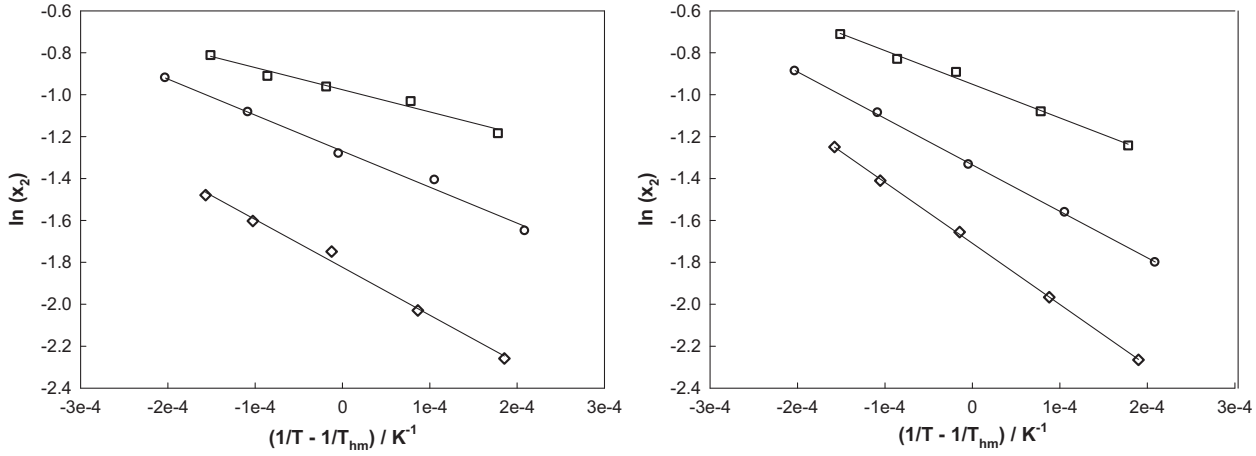

FIGURE 6. $\ln(x_2)$ *vs* $(1/T - 1/T_{hm})$ representation for systems with sorbitol (left) and xylitol (right). [emim][$EtSO_4$], ○; Aliquat®336, □; and Aliquat®[NO_3], ◇.

TABLE 9
Thermodynamic functions of dissolution.

Ionic liquid	Solute	T_{hm}/K	$\Delta^0_{dissol.}H/(\mathrm{kJ}\cdot\mathrm{mol}^{-1})$	$\Delta^0_{dissol.}G/(\mathrm{kJ}\cdot\mathrm{mol}^{-1})$	$\Delta^0_{dissol.}S/(\mathrm{J}\cdot\mathrm{mol}^{-1}\cdot\mathrm{K}^{-1})$
[emim][$EtSO_4$]	Xylitol	307.8	18.4	3.42	48.8
	Sorbitol	307.8	14.3	3.25	35.9
Aliquat®336	Xylitol	326.0	13.4	2.58	33.1
	Sorbitol	326.0	8.8	2.65	18.8
Aliquat®[NO_3]	Xylitol	327.1	24.2	4.57	60.1
	Sorbitol	326.7	19.0	4.87	43.2

$$\Delta^0_{dissol.}G = -RT_{hm}k, \tag{12}$$

where the constant k, is the y-axis intercept of the linear plot represented on figure 6.

Finally, through the definition of Gibbs free energy, one can calculate the entropy of dissolution, $\Delta^0_{dissol.}S$:

$$\Delta^0_{dissol.}S = \frac{\Delta^0_{dissol.}H - \Delta^0_{dissol.}G}{T_{hm}}. \tag{13}$$

Table 9 presents the thermodynamic functions for the six binary systems studied in this work. As the solubility increases with temperature, the obtained dissolution enthalpy, $\Delta^0_{dissol.}H$, shows positive values for all the systems, presenting an endothermic behavior in these dissolution processes. The lower this enthalpy, the easier it is for the system to overcome the energetic barrier for the dissolution. Dissolution entropy plays also an important role as an indicator if solvent molecules' configuration after dissolution is favorable or not. The positive values for $\Delta^0_{dissol.}S$ obtained in all cases indicate a higher mobility of the ionic liquids when they are solvating molecules of carbohydrates than they have in a pure state. The positive values of $\Delta^0_{dissol.}G$ show these dissolution processes are all non-spontaneous, requiring a continuous energy supply to dissolution occurs.

4. Conclusions

Solubilities of xylitol and sorbitol in three ionic liquids were measured over the temperature range of 288 K to 433 K, using an isothermal technique and liquid chromatography. In addition, the densities of the ionic liquids were determined on a vibrating tube densimeter, in a wide temperature range. Measured density of [emim][$EtSO_4$] is in excellent agreement with literature data. Therefore, for Aliquat®336 and Aliquat®[NO_3], their densities at a specific water content were measured for a wide range of temperatures to increase the knowledge on volumetric data of these two ionic liquids, which is still very scarce. Density data were satisfactorily correlated using both linear regression and equation of state for liquids, considering thermal expansion independent of temperature. Both sugar alcohols showed higher solubilities in [emim][$EtSO_4$], where sorbitol is slightly more soluble than xylitol. Solubility in Aliquat's ILs is clearly lower than in [emim][$EtSO_4$], due to the hydrophobic character of this cation. Chloride anion, as a more electron-donor species, provides a higher ability to dissolve carbohydrates than nitrate. Local composition models (NRTL, UNIQUAC, and e-NRTL) were successfully applied to correlate the experimental solubility data. The NRTL's extension to electrolytes presented a slightly better accuracy than the other two models in almost all cases. Thermodynamic functions of dissolution were obtained from the experimental data, showing the dissolution processes of the studied systems are non-spontaneous, endothermic and favorable under an entropic perspective.

Acknowledgements

This work is partially supported by Project PEst-C/EQB/LA0020/2011, financed by FEDER through COMPETE – Programa Operacional Factores de Competitividade and by FCT – Fundação para a Ciência e a Tecnologia. A.C. and O.R. acknowledge financial support (Grant SFRH/BD/62105/2009) and Programme Ciência 2007, respectively, from Fundação para a Ciência e a Tecnologia (FCT, Portugal).

References

[1] B. Kamm, M. Kamm, Appl. Microbiol. Biotechnol. 64 (2004) 137–145.
[2] L.R. Lynd, C.E. Wyman, T.U. Gerngross, Biotechnol. Prog. 15 (1999) 777–793.
[3] Y.H.P. Zhang, J. Ind. Microbiol. Biotechnol. 35 (2008) 367–375.
[4] N. Mosier, C. Wyman, B. Dale, R. Elander, Y.Y. Lee, M. Holtzapple, M. Ladisch, Bioresour. Technol. 96 (2005) 673–686.
[5] Y.H.P. Zhang, M.E. Himmel, J.R. Mielenz, Biotechnol. Adv. 24 (2006) 452–481.
[6] P. Kumar, D.M. Barrett, M.J. Delwiche, P. Stroeve, Ind. Eng. Chem. Res. 48 (2009) 3713–3729.
[7] S.S.Y. Tan, D.R. MacFarlane, Top. Curr. Chem. 290 (2009) 311–339.
[8] S.D. Nicholas, F. Smith, Nature 161 (1948) 349.
[9] G. Bartoli, R. Dalpozzo, A. De Nino, L. Maiuolo, M. Nardi, A. Procopio, A. Tagarelli, Green Chem. 6 (2004) 191–192.
[10] C.D. Hurd, O.E. Edwards, J. Org. Chem. 14 (1949) 680–691.
[11] Z.J. Wei, Y. Li, D. Thushara, Y.X. Liu, Q.L. Ren, J. Taiwan Inst, Chem. Eng. 42 (2011) 363–370.
[12] H. McGuigan, Am. J. Physiol. 19 (1907) 175–198.
[13] E.O. Odebunmi, S.O. Owalude, J. Iran Chem. Soc. 5 (2008) 623–630.
[14] P. Karrer, H. Salomon, R. Kunz, A. Seebach, Helv. Chim. Acta 18 (1935) 1338–1342.
[15] B. Kusserow, S. Schimpf, P. Claus, Adv. Synth. Catal. 345 (2003) 289–299.
[16] J. Wisniak, R. Simon, Ind. Eng. Chem. Prod. Rd. 18 (1979) 50–57.
[17] T.A. Werpy, G. Petersen, Top Value Added Chemicals From Biomass: I. Results of Screening for Potential Candidates from Sugars and Synthesis Gas, Pacific Northwest National Laboratory, 2004.
[18] B.W. Chun, B. Dair, P.J. Macuch, D. Wiebe, C. Porteneuve, A. Jeknavorian, Appl. Biochem. Biotechnol. 131 (2006) 645–658.
[19] J.F. Brennecke, E.J. Maginn, AIChE J. 47 (2001) 2384–2389.
[20] K.R. Seddon, J. Chem. Technol. Biotechnol. 68 (1997) 351–356.
[21] J.G. Huddleston, H.D. Willauer, R.P. Swatloski, A.E. Visser, R.D. Rogers, Chem. Commun. (1998) 1765–1766.
[22] T. Welton, Coord. Chem. Rev. 248 (2004) 2459–2477.
[23] C.M. Gordon, M.J. Muldoon, M. Wagner, C. Hilgers, J.H. Davis, P. Wasserscheid, Synthesis and Purification, Ionic Liquids in Synthesis, Wiley-VCH Verlag GmbH & Co. KGaA, 2008.
[24] S. Zhang, N. Sun, X. He, X. Lu, X. Zhang, J. Phys. Chem. Ref. Data 35 (2006) 1475.
[25] H. Zhao, S. Xia, P. Ma, J. Chem. Technol. Biotechnol. 80 (2005) 1089–1096.
[26] L.F. Vega, O. Vilaseca, F. Llovell, J.S. Andreu, Fluid Phase Equilib. 294 (2010) 15–30.
[27] N.V. Plechkova, K.R. Seddon, Chem. Soc. Rev. 37 (2008) 123–150.
[28] S. Aparicio, M. Atilhan, F. Karadas, Ind. Eng. Chem. Res. 49 (2010) 9580–9595.
[29] Accelerating Ionic Liquid Commercialization, Research Needs to Advance New Technology, BCS Incorporated, 2004.
[30] T.A.D. Nguyen, K.R. Kim, S.J. Han, H.Y. Cho, J.W. Kim, S.M. Park, J.C. Park, S.J. Sim, Bioresour. Technol. 101 (2010) 7432–7438.
[31] K. Shill, S. Padmanabhan, Q. Xin, J.M. Prausnitz, D.S. Clark, H.W. Blanch, Biotechnol. Bioeng. 108 (2011) 511–520.
[32] F.R. Tao, H.L. Song, L.J. Chou, Carbohydr. Res. 346 (2011) 58–63.
[33] F. Jiang, D. Ma, X.H. Bao, Chin. J. Catal. 30 (2009) 279–283.
[34] C.Z. Li, Z.K.B. Zhao, Adv. Synth. Catal. 349 (2007) 1847–1850.
[35] T. Stahlberg, W.J. Fu, J.M. Woodley, A. Riisager, Chemsuschem 4 (2011) 451–458.
[36] S.H. Lee, D.T. Dang, S.H. Ha, W.-J. Chang, Y.-M. Koo, Biotechnol. Bioeng. 99 (2008) 1–8.

[37] N. Sun, H. Rodriguez, M. Rahman, R.D. Rogers, Chem. Commun. 47 (2011) 1405–1421.
[38] R.C. Remsing, G. Hernandez, R.P. Swatloski, W.W. Massefski, R.D. Rogers, G. Moyna, J. Phys. Chem. B 112 (2008) 11071–11078.
[39] H. Renon, J.M. Prausnitz, AIChE J. 14 (1968) 135–144.
[40] C.C. Chen, H.I. Britt, J.F. Boston, L.B. Evans, AIChE J. 28 (1982) 588–596.
[41] D.S. Abrams, J.M. Prausnitz, AIChE J. 21 (1975) 116–128.
[42] J.D. Holbrey, W.M. Reichert, R.P. Swatloski, G.A. Broker, W.R. Pitner, K.R. Seddon, R.D. Rogers, Green Chem. 4 (2002) 407–413.
[43] A.P. Carneiro, O. Rodríguez, E.A. Macedo, Fluid Phase Equilib. 314 (2012) 22–28.
[44] J.P. Mikkola, P. Virtanen, R. Sojholm, Green Chem. 8 (2006) 250–255.
[45] E. Gomez, B. Gonzalez, N. Calvar, E. Tojo, A. Dominguez, J. Chem. Eng. Data 51 (2006) 2096–2102.
[46] A. Fernández, J.n. García, J.S. Torrecilla, M. Oliet, F. Rodríguez, J. Chem. Eng. Data 53 (2008) 1518–1522.
[47] C.L. Wong, A.N. Soriano, M.H. Li, Fluid Phase Equilib. 271 (2008) 43–52.
[48] T. Hofman, A. Goldon, A. Nevines, T.M. Letcher, J. Chem. Thermodyn. 40 (2008) 580–591.
[49] P.S. Kulkarni, L.C. Branco, J.G. Crespo, M.C. Nunes, A. Raymundo, C.A.M. Afonso, Chem. – Eur. J. 13 (2007) 8478–8488.
[50] M.G. Freire, A.R.R. Teles, M.A.A. Rocha, B. Schroder, C.M.S.S. Neves, P.J. Carvalho, D.V. Evtuguin, L.M.N.B.F. Santos, J.A.P. Coutinho, J. Chem. Eng. Data 56 (2011) 4813–4822.
[51] C. Kolbeck, T. Cremer, K.R.J. Lovelock, N. Paape, P.S. Schulz, P. Wasserscheid, F. Maier, H.P. Steinruck, J. Phys. Chem. B 113 (2009) 8682–8688.
[52] B. Tong, Z.-C. Tan, Q. Shi, Y.-S. Li, D.-T. Yue, S.-X. Wang, Thermochim. Acta 457 (2007) 20–26.
[53] C.L. Yaws, Yaws' Handbook of Thermodynamic and Physical Properties of Chemical Compounds, Knovel, 2003.
[54] F.M. Maia, O. Rodriguez, E.A. Macedo, Fluid Phase Equilib. 296 (2010) 184–191.
[55] L.D. Simoni, Y. Lin, J.F. Brennecke, M.A. Stadtherr, Ind. Eng. Chem. Res. 47 (2008) 256–272.
[56] J.M. Prausnitz, R.N. Lichtenthaler, E.G. Azevedo, Molecular Thermodynamics of Fluid-Phase Equilibria, third ed., Prentice Hall, New Jersey, 1999.
[57] Y.H. Song, C.C. Chen, Ind. Eng. Chem. Res. 48 (2009) 7788–7797.
[58] U. Domanska, L. Mazurowska, Fluid Phase Equilib. 221 (2004) 73–82.
[59] V.H. Alvarez, M. Aznar, J. Chin. Inst. Chem. Eng. 39 (2008) 353–360.
[60] S.O. Jonsdottir, S.A. Cooke, E.A. Macedo, Carbohydr. Res. 337 (2002) 1563–1571.
[61] G.M. Kontogeorgis, G.K. Folas, Thermodynamic Models for Industrial Applications, John Wiley & Sons Ltd., 2010.
[62] R.R. Krug, W.G. Hunter, R.A. Grieger, J. Phys. Chem. 80 (1976) 2341–2351.
[63] G.V.S.M. Carrera, C.A.M. Afonso, L.C. Branco, J. Chem. Eng. Data 55 (2010) 609–615.

JCT 12-190